Available online at www.sciencedirect.com

SCIENCE DIRECT®

Cement and Concrete Research 35 (2005) 658–670

CEMENT AND CONCRETE RESEARCH

# Resistance of geopolymer materials to acid attack

T. Bakharev*

*Department of Civil Engineering, Monash University, Wellington Road, Clayton, Victoria 3168, Australia*

Received 23 June 2003; accepted 3 June 2004

## Abstract

This article presents an investigation into durability of geopolymer materials manufactured using a class F fly ash (FA) and alkaline activators when exposed to 5% solutions of acetic and sulfuric acids. The main parameters studied were the evolution of weight, compressive strength, products of degradation and microstructural changes. The degradation was studied using X-ray diffraction (XRD), Fourier transform infrared spectroscopy (FTIR) and scanning electron microscopy (SEM). The performance of geopolymer materials when exposed to acid solutions was superior to ordinary Portland cement (OPC) paste. However, significant degradation of strength was observed in some geopolymer materials prepared with sodium silicate and with a mixture of sodium hydroxide and potassium hydroxide as activators. The deterioration observed was connected to depolymerisation of the aluminosilicate polymers in acidic media and formation of zeolites, which in some cases lead to a significant loss of strength. The best performance was observed in the geopolymer material prepared with sodium hydroxide and cured at elevated temperature, which was attributed to a more stable cross-linked aluminosilicate polymer structure formed in this material.

*Keywords:* Fly Ash; Alkali-activated cement; Durability; Acid attack

## 1. Introduction

Acid resistance is a desirable property for structural materials used in the aggressive environment of chemical, mining, mineral processing and other industries. Basic in nature, concretes made with Portland cement and alkali-activated slag deteriorate in the acid environment [1,2]. In the case of acid attack on ordinary Portland cement (OPC) concrete, calcium salts of the attacking acid rapidly form and the concrete loses its strength and deteriorates quickly. When tested in acetic acid solution of pH 4 for 12 months, AAS concrete had about 33% strength reduction as compared to 47% reduction in OPC. Thus, AAS was found superior in durability to OPC. Its good performance was attributed to low Ca content ( ~ 40% CaO) compared to Portland cement ( ~ 65% CaO) and the glassy state of the slag, which is poorly soluble in the acid solution [2]. Geopolymer materials prepared with the class F fly ash (FA) contain very low calcium (3–4% CaO) and it could be expected that they possess high durability in the acid environment.

Geopolymers are synthetic minerals belonging to the same family of aluminosilicates as zeolites, but unlike zeolites, they are essentially amorphous polymers. The properties of these geopolymer materials prepared using FA are not well studied but there are reports of superior durability and heat-resistant properties of geopolymer materials prepared using metakaolin [3–5]. Geopolymer materials are produced by a sol–gel process utilising alumina and silica oxides activated by alkali hydroxides and/or alkali silicates. The starting materials dissolve in high pH alkaline solution and the geopolymers are precipitated; this process being facilitated by heat. In the process of the polymerisation reactions, polysialates, polysialate siloxo, and polysialate disiloxo are formed [3]. The mineral polymers have empirical formula: $M_n[-(SiO_2)_z-AlO_2]_n \cdot wH_2O$, where $z$ is 1, 2 or 3; M is an alkali cation, such as potassium or sodium, and $n$ is the degree of polymerisation [4,5]. In a previous article, the processing and characterisation of geopolymer materials made using class F FA and formed at elevated temperature were discussed [6]. This article presents a study of durability in the acid environment of three geopolymer materials utilising class F FA activated by sodium silicate, sodium hydroxide and a mixture of sodium and potassium hydroxides.

---

* Tel.: +61-3-9905-5549; fax: +61-3-9905-4944.
*E-mail address:* tanya.bakharev@eng.monash.edu.au (T. Bakharev).

0008-8846/$ – see front matter © 2004 Elsevier Ltd. All rights reserved.
doi:10.1016/j.cemconres.2004.06.005

## 2. Experimental

### 2.1. Materials

The chemical and mineral compositions of FA are shown in Table 1 and Fig. 1, respectively. FA used was sourced from Gladstone in Queensland, Australia. It is mainly glassy with some crystalline inclusions of mullite, hematite and quartz. Laboratory grade sodium silicate solution type D with Ms (ratio of silica to sodium oxide) equal to 2, and 14.7% $Na_2O$ and 29.4% $SiO_2$ was supplied by PQ Australia, while 60% w/v sodium hydroxide solution was supplied by Sigma. Potassium hydroxide pellets were supplied by Aldrich. Sodium hydroxide, potassium hydroxide, and sodium silicate solutions were used for FA activation.

### 2.2. Test procedures

FA was activated by sodium hydroxide, a mixture of sodium and potassium hydroxides and sodium silicate solutions, providing 8–9% Na in the mixtures and water/binder (w/b) ratio of 0.3. The preparation process and composition of the investigated materials were developed in a previous article [6]. Concentration of alkalis and w/b ratio in the materials was similar to corresponding numbers of geopolymer materials studied in [7–9]. Table 2 shows the details of the samples and curing conditions. The pastes were cast in plastic cylinders and sealed with the lid. The mixtures were cured for 24 h at room temperature, after which temperature was ramped to 95 °C and maintained at this level for 24 h. The materials were then cooled down to room temperature in the oven for 2 days, and initial compressive strengths was determined (8FAK, 56–58 MPa; 8FASS, 66 MPa; 8FA, 57–59.5 MPa). The samples were then exposed to immersion tests.

The resistance of materials to acid attack was studied by immersion of cylindrical specimens (∅25 × 50 mm) in 5% solutions of acetic and sulfuric acids. The strength of acid solutions used in the test was not equal. The solution of sulfuric acid had pH 0.8 and was much stronger than solution of acetic acid, which had pH of 2.4. The choice of acids solutions and their concentrations were based on practical utilisation of concrete as a construction material in sewage pipes, mining, and food processing industries. The testing media were replaced monthly with fresh solutions. The compressive strength of cylinders (∅25 × 50 mm) was measured at 30, 60, 90, 120 and 150 days of exposure. Neat Portland cement paste (OPC) and Portland cement paste with 20% FA replacement (OPC + FA) with w/b ratio 0.4 were used for comparison in the tests. The specimens containing Portland cement at w/b = 0.4 had the same consistency as the geopolymer specimens at w/b = 0.3. Thus, the specimens were compared as having the same consistency at the time of moulding. The compressive strengths of OPC and OPC + FA specimens at the age of 2 months, when they were used in immersion tests, were 45 and 42.9 MPa, respectively.

The deterioration was studied by X-ray diffraction (XRD), Fourier transform infrared spectroscopy (FTIR) and scanning electron microscopy (SEM). For the analysis, the samples were taken from the surface (1–2 mm depth) exposed to solutions. XRD analyses were made using a Rigaku Geigerflex D-max II automated diffractometer with the following conditions: 40 kV, 22.5 mA, Cu–Kα radiation. The XRD patterns were obtained by scanning at 0.1° ($2\theta$) per min and in steps of 0.05° ($2\theta$). SEM (Hitachi S-2300, Japan) was used for microstructural observations of the fracture surfaces, which were coated with evaporated gold for examination in the secondary electron mode. FTIR was performed on the samples using a Perkin Elmer 1600 spectrometer and the KBr pellet technique (3 mg powder sample mixed with 100 mg KBr).

## 3. Results

Geopolymer specimens had very small change in appearance after 5 months of immersion in the acidic solutions. Some softening of the surface cover and insignificant lightening of the colour could be noticed in the 8FA, 8FASS and 8FAK geopolymer specimens after exposure to the solution of sulfuric acid. In the acetic acid, there was no change in appearance of 8FAK specimens and very small change in appearance of 8FASS and 8FA specimens.

Visual examination of specimens exposed to the sulfuric acid solution showed severe deterioration of the OPC and OPC + FA specimens that is consistent with high content of calcium in these samples. Within days, OPC samples had a thick layer of white paste formed on the surface. After 2 weeks, the surface layer of the samples was converted to some reaction products to a depth of 8 mm. After 1 month, OPC samples were severely deteriorated. The surface layer

Table 1
Composition of dry materials (mass %) by XRF

| Oxide | $SiO_2$ | $Al_2O_3$ | $Fe_2O_3$ | CaO | MgO | $K_2O$ | $Na_2O$ | $TiO_2$ | $P_2O_5$ | MnO | $SO_3$ | Loss on ignition |
|---|---|---|---|---|---|---|---|---|---|---|---|---|
| FA[a] | 50.0 | 28.0 | 12.0 | 3.5 | 1.3 | 0.7 | 0.2 | 3.2 | 0.42 | 0.03 | 0.12 | 0.53 |
| Portland cement[b] | 19.9 | 4.62 | 3.97 | 64.27 | 1.73 | 0.57 | 0.15 | 0.23 | 0.12 | 0.06 | 2.56 | 2.9 |

[a] Pozzolanic Enterprises, Port Melbourne, Australia.
[b] Type I/II, Geelong, Victoria, Australia.

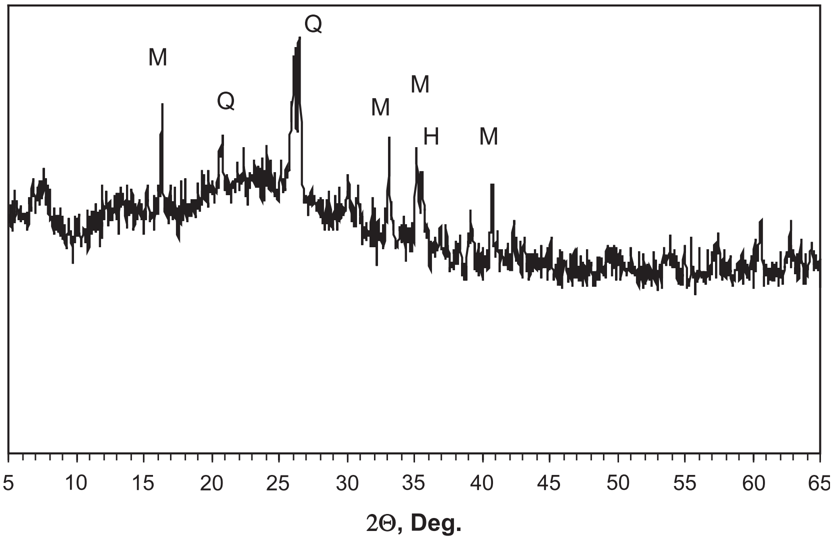

Fig. 1. XRD traces of FA. Q = quartz, M = mullite, H = hematite.

of OPC + FA samples deteriorated to a depth of 4 mm after 1 month and 10 mm after 3 months. In acetic acid solution, there was a significant loss of cement paste material from the surface in OPC specimens and change in the colour of the surface layer in OPC + FA specimens.

Table 3 gives the weight changes for the specimens exposed to acidic solutions for 2 months. The most significant weight change in both acetic and sulfuric acids was in OPC and OPC + FA samples, which had weight losses in acetic acid solution of 10% and 5.47%, respectively. In sulfuric acid, both OPC and OPC + FA samples had weight gain. OPC samples gained more than 40% and severely deteriorated, while OPC + FA samples gained 19.15% and exhibited severely deteriorated surface layer.

Among geopolymer samples, the best performance in both tests was by samples activated by sodium hydroxide, which had weight losses in acetic and sulfuric acid solutions of 0.45% and 1.96%, respectively. Next in performance were samples activated by sodium silicate solution, which had 3.83% weight gain in the acetic acid solution and 2.56% weight loss in the sulfuric acid solution. The performance of the samples prepared with sodium hydroxide and potassium hydroxide solutions was good in acetic acid solution with 1.15% weight loss, but rather poor in sulfuric acid solution with 12.43% weight loss.

### 3.1. Compressive strength

Fig. 2 shows the evolution of the compressive strength of the samples exposed to the acetic acid solution. The 8FAK samples activated by sodium and potassium hydroxide solution performed well with 4.5% strength loss in the first month and about 10% strength decline in the second month of exposure, which continued over the next 4 months, reaching 38.3% after 6 months of the test. Next in performance were 8FA samples activated by sodium hydroxide solution, which had a rapid strength loss of about 45% after 2 months of exposure, but recovered slightly and had about 40% strength reduction after 6 months of the test. 8FASS samples activated by sodium silicate had about 60% strength decline after 6 months of exposure. Polynomial trend lines were used to show the trend of strength evolution in 8FA and 8FASS specimens, because very significant fluctuations of strength were observed in these two materials in the acetic acid solution. OPC and OPC + FA paste samples had 91% and 69% strength loss, respectively, after 2 months, and about 91% and 84%, respectively, after 6 months of exposure. Significant fluctuations of strength

Table 2
Alkali-activated FA samples

| Sample | Type of activator and w/b ratio | Concentration | Curing conditions |
|---|---|---|---|
| 8FASS | Sodium silicate, w/b = 0.3 | 8% Na | |
| 8FA | Sodium hydroxide, w/b = 0.3 | 8% Na | 24 h at room temperature, 24 h at 95 °C for all cases |
| 8FAK | Sodium hydroxide + potassium hydroxide, w/b = 0.3 | 8%Na and 1% K | |

Table 3
Weight changes of the samples exposed to 5% solutions of sulfuric and acetic acids

| Sample | Acetic acid (%) | Sulfuric acid (%) |
|---|---|---|
| OPC | − 10 | >40 |
| OPC + FA | − 5.47 | 19.15 |
| 8FA | − 0.45 | − 1.96 |
| 8FASS | 3.83 | − 2.56 |
| 8FAK | − 1.15 | − 12.43 |

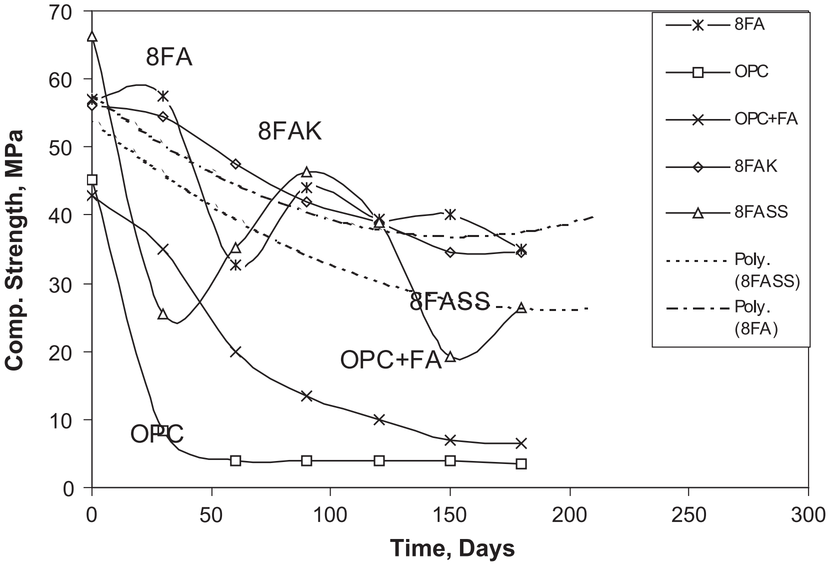

Fig. 2. Compressive strength evolution of the geopolymer and Portland cement specimens exposed to 5% acetic acid solution.

measured in 8FASS and 8FA specimens were possibly connected to the breakdown of some geopolymer components and migration of alkalis from the specimens into solution superimposed by the acid attack.

Fig. 3 shows the evolution of the compressive strength of the samples exposed to the sulfuric acid solution. The 8FA samples activated by sodium hydroxide had the best performance with 6.4% strength decline in the first month of the test and additional 4% strength decline every month afterward. The 8FA samples had 17.5% strength loss after 4 months of the test and the strength of the specimens was stabilised afterward. The 8FAK and 8FASS samples had very small change in appearance, but the samples had 89% and 82% strength loss, respectively, after 2 months of the test. The OPC samples completely deteriorated in the first month of the test and OPC + FA samples had 77% strength loss and were severely deteriorated.

### *3.2. X-ray diffraction*

Fig. 4 shows XRD pattern of the geopolymer samples before the test. Peaks due to quartz, mullite and hematite of the crystalline component of the FA can be seen in addition to the broad peak in the region 20–32° $2\theta$ arising from the glassy phase of the FA and broad peak in the region 6–10° $2\theta$ arising from aluminosilicate gel. In addition, peaks for hydroxysodalite and Na–P1 (gismondine) zeolites were present in the XRD spectra of the 8FA and 8FAK specimens. The 8FA specimen contained more ordered hydroxysodalite and Na–P1 (gismondine) zeolites than 8FAK specimen.

Fig. 5 shows the XRD spectra of the geopolymer materials exposed to the acetic acid solution for 2 months. Traces of hydroxysodalite and Na–P1 zeolites disappeared in the XRD spectrum of 8FA, and a broad peak in the region 11–20° $2\theta$, attributed to amorphous aluminosilicate gel,

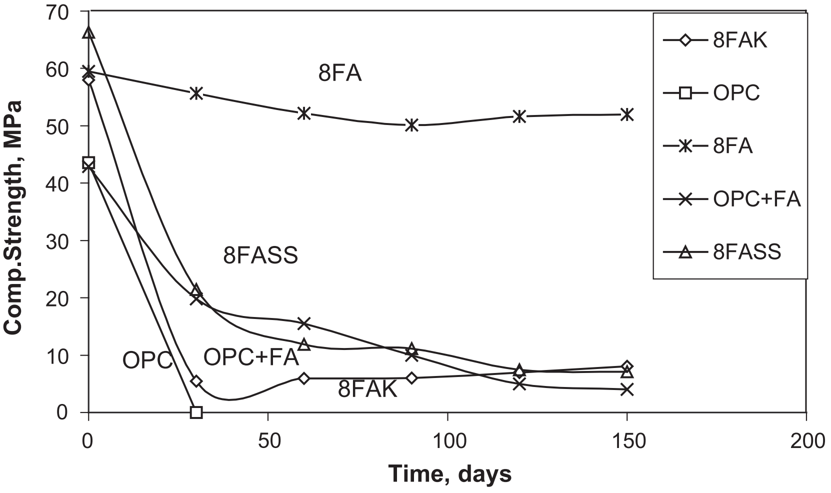

Fig. 3. Compressive strength evolution of the geopolymer and Portland cement specimens exposed to 5% sulfuric acid solution.

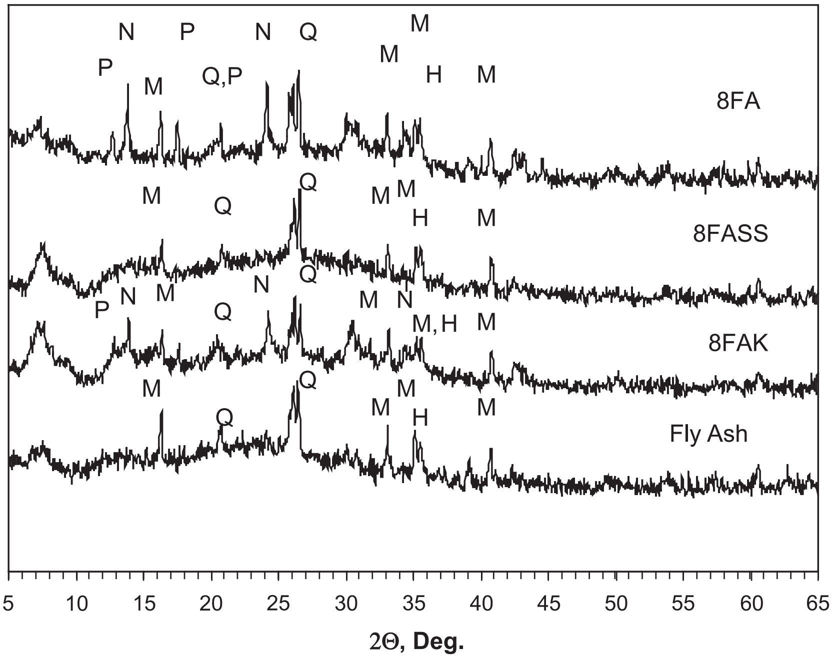

Fig. 4. XRD analysis of the geopolymer materials before tests: (a) 8FA, (b) 8FASS, and (c) 8FAK. P = Na–P1 (gismondine), N = hydroxysodalite, Q = quartz, M = mullite, H = hematite.

was observed instead. The 8FAK specimen underwent significant changes when exposed to acetic acid solution. A broad peak in the region 7–10° $2\theta$ arising from the amorphous aluminosilicate gel dominates the XRD spectrum after the immersion test. It is suggested that disappearance of peaks of quartz and some other crystalline residue of FA in the pattern of 8FAK specimen is due to the crystal surface being covered by amorphous phases formed as a result of the reaction of aluminosilicate gel with acetic acid solution, thereby masking the XRD reflections that would have otherwise been generated by these minerals. There were only small changes in the XRD spectrum of 8FASS after the exposure to the acetic acid solution.

Fig. 6 presents XRD spectra of the geopolymer materials exposed to 5% sulfuric acid solution for 2 months. The 8FA specimen has undergone significant changes by exposure to sulfuric acid solution. It can be seen that peaks for zeolitic phases have disappeared, and a broad peak at 7–10° $2\theta$,

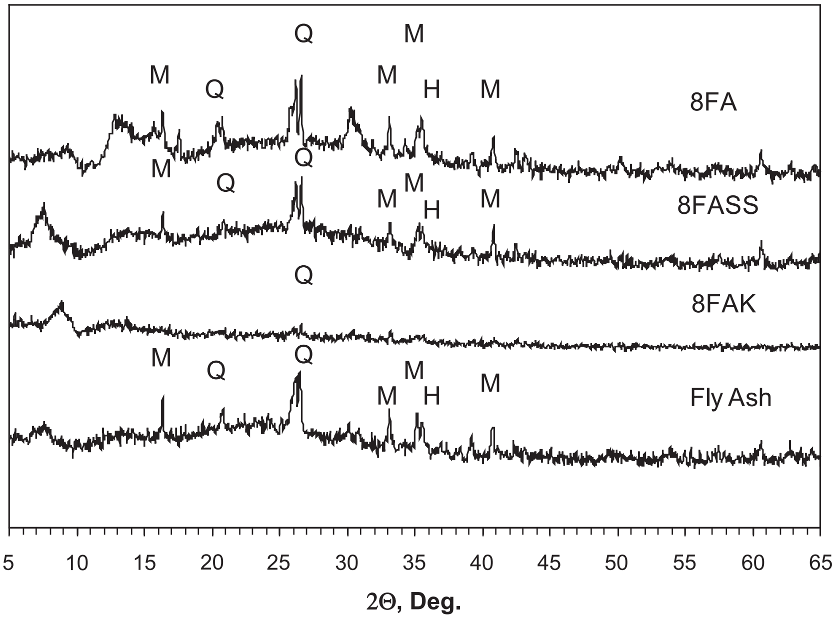

Fig. 5. XRD pattern of the geopolymer materials exposed to 5% acetic acid solution. Q = quartz, M = mullite, H = hematite.

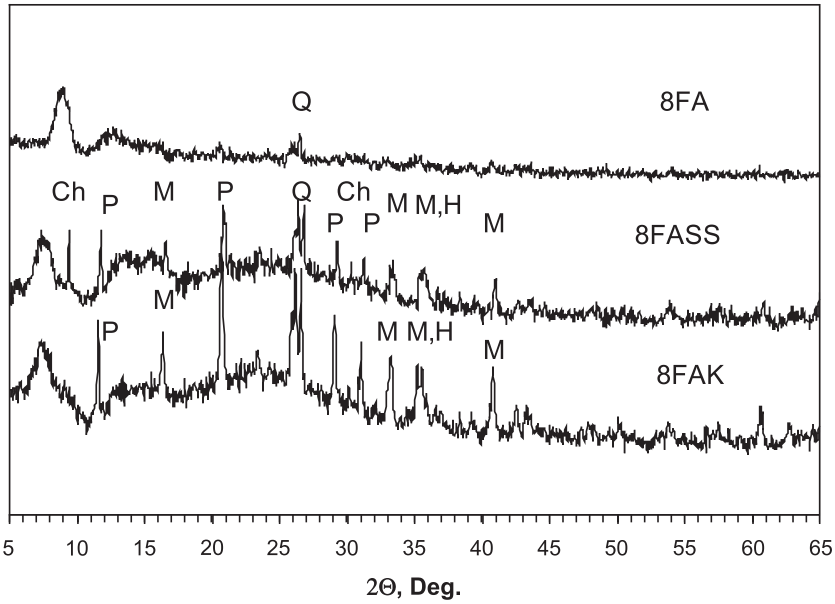

Fig. 6. XRD pattern of the geopolymer materials exposed to 5% sulfuric acid solution. Ch = chabazite, P = Na–P1 (gismondine), Q = quartz, M = mullite, H = hematite.

arising from aluminosilicate gel, dominates the traces. Similar to the case of the acetic acid solution, precipitation of new amorphous phases on the surfaces of quartz, mullite and hematite crystals may cause a reduction of their peak intensities in the XRD pattern. On the contrary, in the spectra of 8FASS and 8FAK some new peaks can be seen

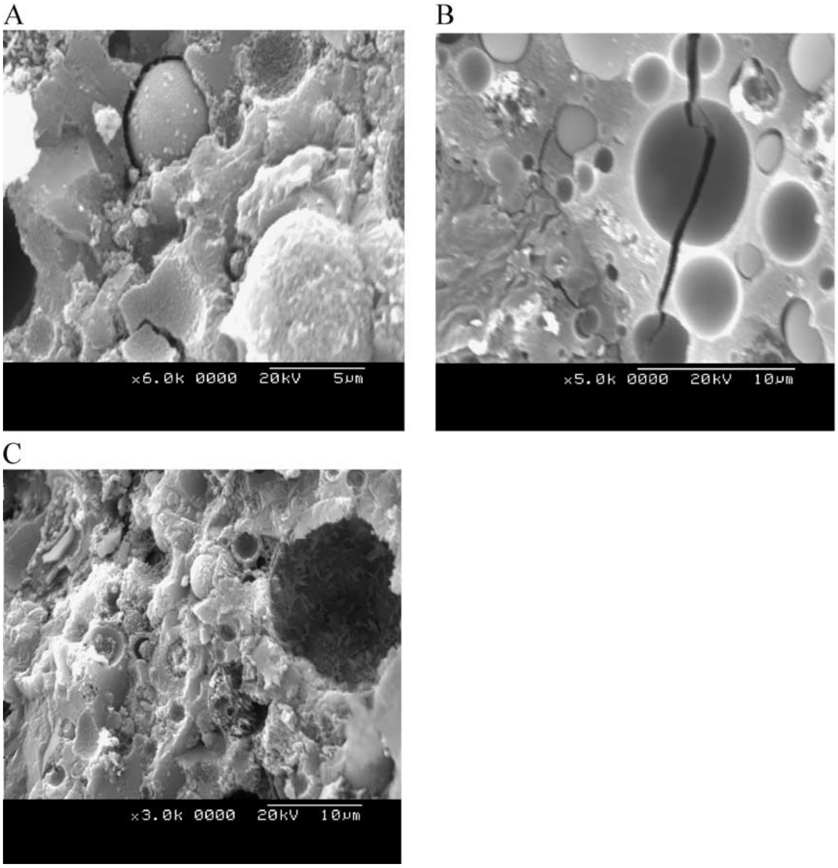

Fig. 7. Representative SEM images of geopolymer samples before the test: (A) 8FA, (B) 8FASS, and (C) 8FAK.

arising from crystalline zeolitic phases. After 2 months of exposure to the sulfuric acid solution, the 8FASS specimen contained chabazite and Na–P1 (gismondine) zeolites, while the 8FAK specimen contained Na–P1 (gismondine) zeolite in addition to the amorphous aluminosilicate gel and crystalline residue of the FA.

### 3.3. Scanning electron microscopy

Fig. 7(A-C) shows SEM images of the 8FA, 8FASS, and 8FAK geopolymer specimens, respectively, before the immersion test. The specimens activated by sodium hydroxide (8FA) had more crystalline appearance, particularly than the specimens activated by sodium silicate (8FASS). Fig. 8(A-C) shows 8FA, 8FASS and 8FAK specimens, respectively, exposed to 5% acetic acid solution for 2 months. The 8FASS and 8FA specimens became porous after exposure to acetic acid (Fig. 8(A,B)). On the contrary, in the 8FAK specimen, no porous structures were observed, but the material had an amorphous appearance after the immersion test with some fissures developed in the surface area (Fig. 8(C)).

Fig. 9(A–C) shows SEM images of the 8FA, 8FASS, and 8FAK geopolymer specimens, respectively, exposed to sulfuric acid solution for 2 months. The specimens exposed to sulfuric acid solutions became very porous and fragile. SEM observations indicated that some new crystals were formed in the matrix of 8FASS and 8FAK specimens. In the 8FA specimen, mainly amorphous structures can be seen after 2 months of exposure. Some fissures similar to Fig. 8(C) developed in the surface area of the 8FA specimens exposed to sulfuric acid solution.

### 3.4. Fourier transform infrared spectroscopy

Figs. 10–12 present IR spectra of the geopolymer materials before the immersion test and after exposure to acetic acid and sulfuric acid solutions. The identification of the IR spectral bands was performed using zeolite IR assignments given in Ref. [10]. In the materials before the exposure, the strongest vibration at 960–1100 cm$^{-1}$ is assigned to asymmetrical T–O stretch, here T is a silicon atom. The next strongest band at 426 cm$^{-1}$ is assigned to a T–O bending mode. The T–O–T symmetrical stretching vibrations are assigned in 688-cm$^{-1}$ region. The T–OH stretching modes are assigned in the region 850 cm$^{-1}$. Vibrations assigned to double ring are in 520–532 cm$^{-1}$ region. The stretching modes are sensitive to the Si–Al composition of the framework and may shift to a lower frequency with increasing number of tetrahedral aluminium atoms. Thus, asymmetric stretch Al–O–Si was assigned in 960 cm$^{-1}$, while Si–O–

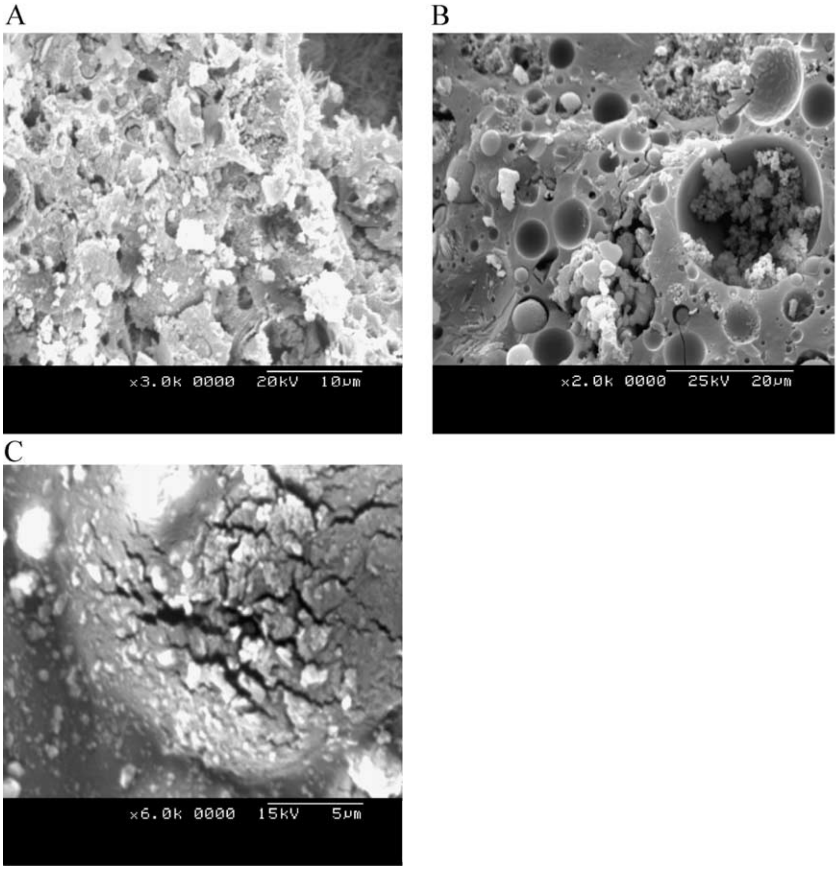

Fig. 8. Representative SEM images of geopolymer samples after 2 months in 5% acetic acid: (A) 8FA, (B) 8FASS, and (C) 8FAK.

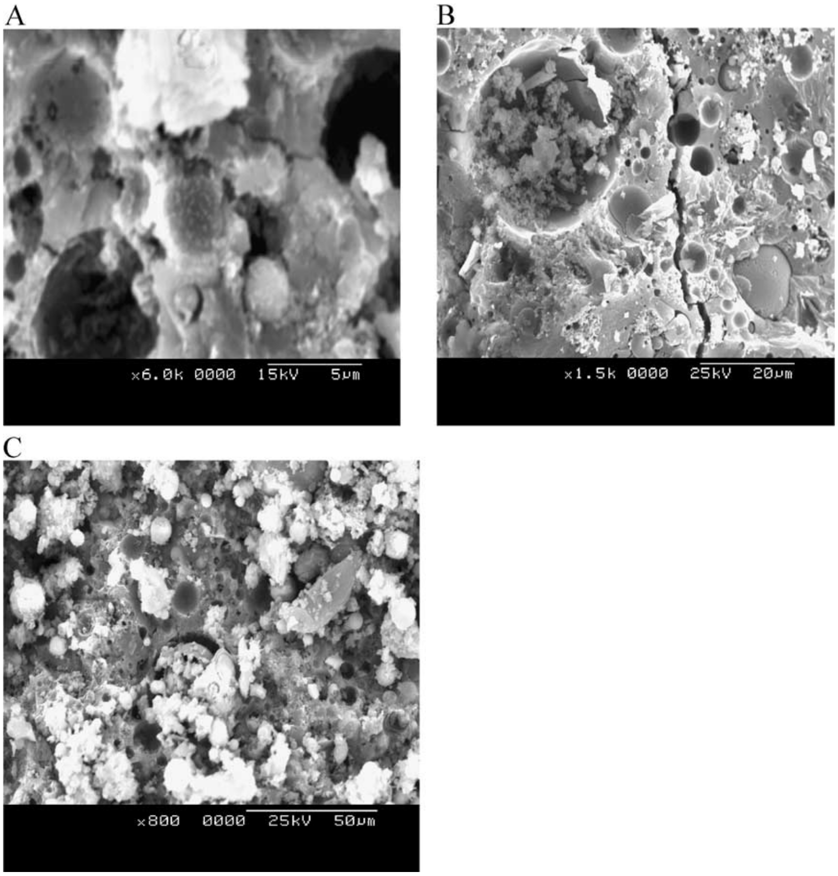

Fig. 9. Representative SEM images of geopolymer samples after 2 month in 5% sulfuric acid solution: (A) 8FA, (B) 8FASS, and (C) 8FAK.

Si stretch was assigned in 1000-cm$^{-1}$ region. The bending mode, that is, the 420–500 cm$^{-1}$ band, is not as sensitive to aluminium substitution.

Exposure to acetic acid produced significant shifts in all the aluminosilicate spectral bands, by comparison with those of the materials before this treatment (Figs. 10–12), e.g.,

(i) The asymmetrical Si–O–Al and Si–O–Si stretching vibrations shifted from 960 and 1026–1120 cm$^{-1}$ to

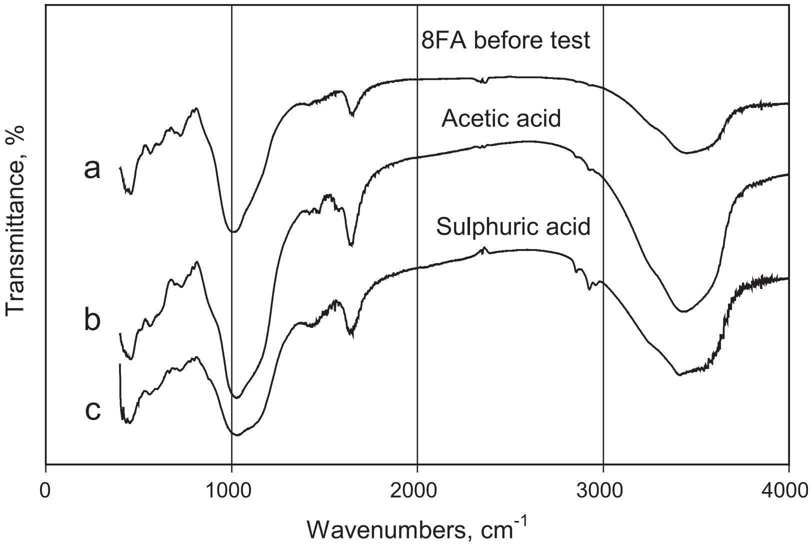

Fig. 10. IR spectra of 8FA specimens (a) before the test, (b) exposed to 5% acetic acid solution for 2 months, and (c) exposed to sulfuric acid solution for 2 months.

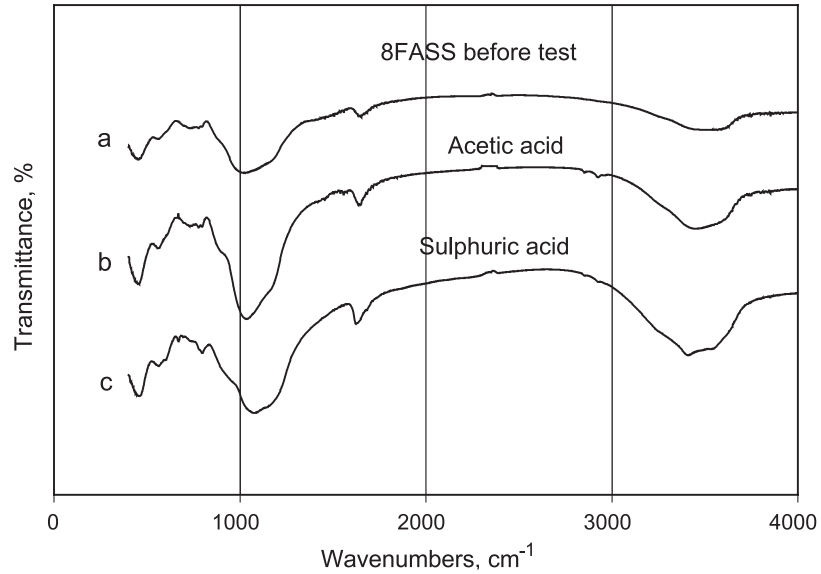

Fig. 11. IR spectra of 8FASS specimens (a) before the test, (b) exposed to 5% acetic acid solution for 2 months, and (c) exposed to sulfuric acid solution for 2 months.

986 and 1080–1130 $cm^{-1}$, respectively, in 8FASS sample; from 976 and 1100 $cm^{-1}$ to 994 and 1064–1118 $cm^{-1}$, respectively, in 8FA sample; shifted from 970 and 1100 $cm^{-1}$ to 986 and 1088–1106 $cm^{-1}$, respectively, in 8FAK sample.

(ii) The Si–OH and Al–OH stretching vibrations in 854 $cm^{-1}$ region became stronger and shifted to 878 and 880 $cm^{-1}$ in 8FA and 8FASS samples, respectively; and to 868 $cm^{-1}$ in 8FAK sample.

(iii) The Si–O–Si and Si–O–Al symmetric stretching vibrations in 688 $cm^{-1}$ region shifted to 704 $cm^{-1}$ in 8FA sample, 664–746 $cm^{-1}$ in 8FASS and 684 $cm^{-1}$ in 8FAK sample.

(iv) The O–Si–O bending vibrations at 426 $cm^{-1}$ shifted to 416 $cm^{-1}$ in 8FA sample and 424 $cm^{-1}$ in 8FAK and had no change in 8FASS sample spectra.

(v) Double-ring vibrations at 520–532 $cm^{-1}$ shifted to 530–602 $cm^{-1}$ in 8FA sample, 520 $cm^{-1}$ in 8FASS, and 520–592 $cm^{-1}$ in 8FAK sample.

To summarise, after exposure to the acetic acid solution, in the 8FA, 8FASS and 8FAK samples, there was an

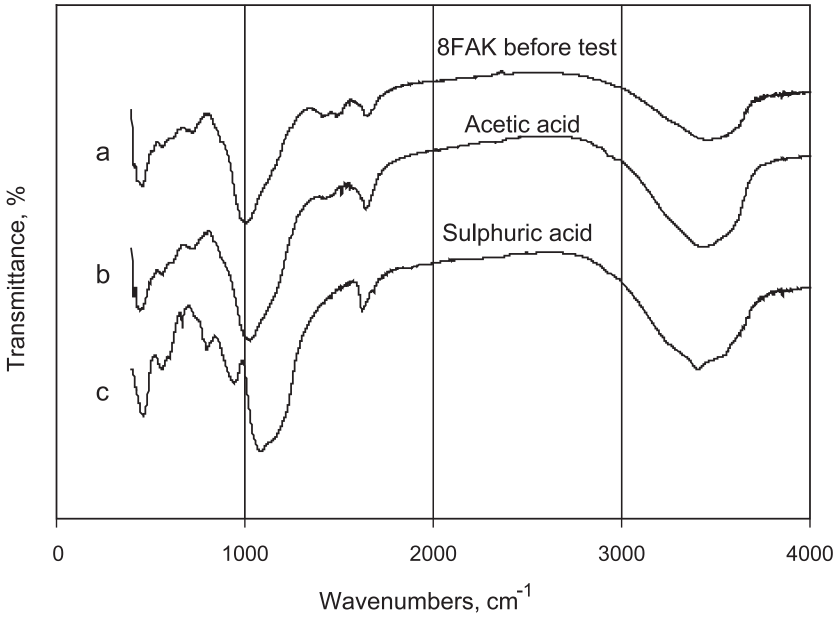

Fig. 12. IR spectra of 8FAK specimens (a) before the test, (b) exposed to 5% acetic acid solution for 2 months, and (c) exposed to 5% sulfuric acid solution for 2 months.

increase of Si/Al atom ratio in the polymers and an increase of the chain length. In addition, there was an increase of the Si–OH and Al–OH groups in 8FA and 8FASS samples. In acetic acid, the least changes were induced in IR spectra of the 8FAK sample.

Exposure to sulfuric acid also produced very significant shifts in the aluminosilicate spectral bands, by comparison with those of the materials before this treatment (Figs. 10–12), e.g.,

(vi) The asymmetrical Si–O–Al and Si–O–Si stretching vibrations shifted from 960 and 1026–1120 cm $^{-1}$ to 1022 and 1056–1130 cm $^{-1}$, respectively, in 8FASS sample; from 976 and 1100 cm $^{-1}$ to 980 and 1046–1170 cm $^{-1}$, respectively, in 8FA sample; from 970 and 1100 cm $^{-1}$ to 1056 and 1062–1152 cm $^{-1}$ respectively, in 8FAK sample.
(vii) The Si–OH and Al–OH stretching vibrations in 854 cm $^{-1}$ region became much stronger and shifted to 916 cm $^{-1}$ in 8FAK sample, 900 cm $^{-1}$ in 8FASS, and had no change in 8FA sample.
(viii) The Si–O–Si and Si–O–Al symmetric stretching vibrations at 688 cm $^{-1}$ shifted to 782 cm $^{-1}$ in 8FAK, 770 cm $^{-1}$ in 8FASS sample, and had no change in 8FA sample.
(ix) The O–Si–O bending vibrations at 426 cm $^{-1}$ became stronger and shifted to 444 and 430 cm $^{-1}$ in 8FAK and 8FASS, respectively, and had no change in 8FA sample.
(x) Double-ring vibrations at 520–532 cm $^{-1}$ shifted to 520–574 cm $^{-1}$ in 8FASS, 542–572 cm $^{-1}$ in 8FAK, and had no change in 8FA sample.
(xi) New band due to sodium sulfate at 636 cm $^{-1}$ appeared in 8FAK and 8FASS samples.

In summary, after exposure to sulfuric acid, there was an increase of the Si/Al atom ratio in the 8FA, 8FASS and 8FAK samples. There was also some increase in the chain length in 8FAK sample. In addition, after treatment by sulfuric acid, concentration of ring silicates and the Si–OH and Al–OH groups significantly increased in 8FAK and 8FASS samples. The least changes were found in the IR spectra of the 8FA sample.

In both acidic solutions, there was an increase in the wave number of the bands in the region of 1600 and 3450 cm $^{-1}$, which were attributed to bending vibrations (H–O–H) and stretching vibration (–OH) due to weakly bound $H_2O$ molecules adsorbed on the surface or trapped in the large cavities.

## 4. Discussion

To understand the process that takes place in the geopolymer materials immersed in the acidic solution, let us start with the reactions that occur in the materials before immersion. The possible chemical processes of dissolution of the starting materials and condensation of silicon and aluminium monomers can be represented as the following reactions [11]:

$$(\text{Al}-\text{Si solid})(\text{fly ash particle}) + OH^{-}(\text{Aq}) \Leftrightarrow \underset{\text{monomer}}{Al(OH)_4^{-}} + \underset{\text{monomer}}{{}^{-}OSi(OH)_3} \qquad (1)$$

$${}^{-}OSi(OH)_3OH^{-} \Leftrightarrow {}^{-}OSi(OH)_2O^{-}_{+}H_2O \qquad (2)$$

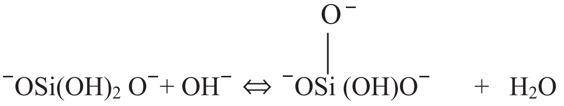

$${}^{-}OSi(OH)_2\,O^{-} + OH^{-} \Leftrightarrow {}^{-}O\overset{\overset{O^{-}}{|}}{Si}(OH)O^{-} + H_2O \qquad (3)$$

$${}^{-}OSi(OH)_3 + M^{+} \Leftrightarrow \underset{\text{monomer}}{M^{+-}OSi(OH)_3} \qquad (4)$$

$${}^{-}OSi(OH)_2O^{-}_{+2}M^{+} \Leftrightarrow \underset{\text{monomer}}{M^{+-}OSi(OH)_2O^{-}M^{+}} \qquad (5)$$

$$\underset{\text{monomer}}{{}^{-}OSi(OH)_3} + M^{+} + \underset{\text{monomer}}{M^{+-}OSi(OH)_3} \Leftrightarrow \underset{\text{dimer}}{M^{+-}OSi(OH)_2 - O - O\;Si(OH)_3} + MOH \qquad (6)$$

$$\underset{\text{monomer}}{{}^{-}OSi(OH)_2\,O^{-}} + M^{+} + \underset{\text{monomer}}{M^{+-}OSi(OH)_3} \Leftrightarrow \underset{\text{dimer}}{M^{+-}OSi(OH)_2 - O - OSi(OH)_2O^{-}} + MOH \qquad (7)$$

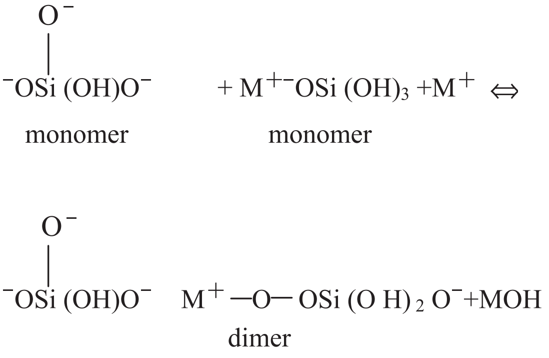

$$\underset{\text{monomer}}{{}^{-}O\overset{\overset{O^{-}}{|}}{Si}(OH)O^{-}} + \underset{\text{monomer}}{M^{+-}OSi(OH)_3} + M^{+} \Leftrightarrow \underset{\text{dimer}}{{}^{-}O\overset{\overset{O^{-}}{|}}{Si}(OH)O^{-}\;M^{+}-O-OSi(OH)_2O^{-}} + MOH \qquad (8)$$

$$2\ \text{Silicate monomer} + 2\ \text{Silicate dimers} + 2\ M^{+} \Leftrightarrow M^{+}\text{cyclic trimer} + M^{+}\text{linear trimer} + 2OH^{-}, \qquad (9)$$

where M is an alkali metal, Na, K.

Reaction (1) describes dissolution reaction for the FA particle, which depends on the pH of the solution, the structure and the surface properties of the FA particle [9]. Eqs. (1)–(3) describe chemical hydration reactions, where the $OH^-$ anions react with the Al–Si solid surface to form $Al(OH)_4^-$, $-OSi(OH)_3$, divalent orthosilicic acid and trivalent orthosilicic acid ions. Reactions (4) and (5) present physical electrostatic reactions, where the alkali metal cation $M^+$ reacts with $Al(OH)_4^-$, $-OSi(OH)_3$, divalent orthosilicic acid and trivalent orthosilicic acid ions to balance Coulombic electrostatic repellence [12]. The cation–anion pair condensation interactions presented by Reactions (6)–(9) lead to condensation of dimer and trimer ions. In the system with sodium silicate activator, more polymerised silicate ions than dimer and trimer may be present, such as tetramer, pentamer, hexamer, octamer, nonamer and their compounds [13]. From the nine reactions given above, it can be seen that decreasing the concentration of the alkaline solution in acidic media favours the equilibrium in these nine reactions shifting to the left-hand side.

In the acidic solution, the concentration of monomer, dimer and trimer ions would increase as a result of shifting the balance in Reactions (1)–(9) to the left-hand side by neutralising the MOH with the acid. In Reactions (6)–(9), a shift of the balance due to reduced pH will induce depolymerisation of the silicate species formed. In addition, in Reactions (4))–(9), $H^+$ ions may substitute for $M^+$, which could change the condensation process. An increased amount of silicic acid ions and dimers will be present in the system. It is in agreement with Iller, who states that in the acidic conditions silicic acid may be liberated from silicates, which contain unpolymerised $SiO_4$ tetrahedra [14]. In the sulfuric acid solution, we observe formation of amorphous silica outside the geopolymeric samples. Iller states that silicic acid is most stable at pH 2–3. However, ageing of a supersaturated solution of silicic acid produces a “solid” phase of amorphous silica. This silica appears in a form of colloidal particles, a precipitate or a gel. The polymerisation of silicic acid involves the condensation of silanol (SiOH) groups to form siloxane (Si–O–Si) bonds [14].

Interaction of geopolymers with the acid solutions can also cause replacement of the exchangeable cations (Na, K) in polymers by hydrogen or hydronium ions [10]:

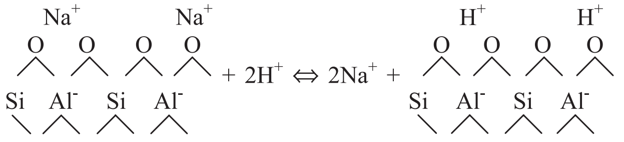

(10)

However, treatment of a geopolymer with a strong acid may result in a direct attack on the aluminosilicate framework and dealumination. This attack will cause breakage of the Si–O–Al bonds, increased number of Si–OH and Al–OH groups in geopolymers and an increased amount of silicic acid ions and dimers in solution. Therefore, this process leads to a mass loss of the geopolymer materials. Polymer structures with a Si/Al ratio of 1 are more subject to the attack by the acid than more siliceous polymers [10].

The observation of the mass changes of the samples exposed to acidic solutions and XRD and FTIR data support the hypothesis of aluminosilicate polymer depolymerisation and liberation of silicic acid from the samples, replacement of Na and K cations by hydrogen or hydronium ion and dealumination of the geopolymer as a result of exposure to acidic solutions. These processes induced mass loss in 8FA and 8FAK samples in both acetic and sulfuric acid solutions. The 8FAK samples experienced very significant 12.4% weight loss in the sulfuric acid solution. Precipitation of silica gel was observed in both 8FAK and 8FA samples in the acid solutions. The 8FASS samples lost weight in sulfuric acid solution. However, 8FASS samples gained weight as the result of reaction with the acetic acid solution. Possibly, products of depolymerisation precipitated as gel or zeolites in the 8FASS sample, thus increasing its weight. Liberation of Na in 8FASS and 8FAK samples in sulfuric acid solution is evident from IR data, which indicated presence of sodium sulfate in the samples subjected to sulfuric acid solution.

IR data show an increase in Si–OH and Al–OH groups concentration resulting from the sulfuric and acetic acid attack on aluminosilicate polymer structure. FTIR observations of the shift of the Si–O–Si asymmetric stretching band at 960–1000 $cm^{-1}$ indicate an increase in the Si/Al ratio in the polymer. The increase of the intensity of the band 980–1100 $cm^{-1}$ indicates an increase of the length of siloxane and aluminosilicate chains. Therefore, in 8FA, 8FASS and 8FAK samples, dealumination of the geopolymers and condensation process caused an increase of the Si/Al ratio and the polymer chain length in the acetic acid solution. However, there was less significant increase in the intensity of the band 980–1100 $cm^{-1}$ in sulfuric acid solution than in acetic acid solution. There was more significant shift in IR spectral bands of 8FA and 8FASS samples caused by immersion in sulfuric acid than in acetic acid solution. Hence, sulfuric acid was more aggressive than acetic acid in its action on geopolymers and caused more severe dealumination and depolymerisation of geopolymers. It is consistent with higher strength of sulfuric acid solution than acetic acid solution used in the test as a medium. In addition, some new zeolitic phases formed in 8FASS and 8FAK samples in the sulfuric acid medium. According to XRD and SEM data, either amorphous polymers, or zeolites are precipitated in geopolymers as a result of exposure to acidic solutions. Thus, in a medium of low pH, depolymerisation of geopolymers is followed by condensation of polymeric ions enriched with silicon. This general description of the processes that take place in the geopolymer materials exposed to acid solutions is modified in each case because of peculiarities of the polymer structure influenced by the type of activator and heat curing procedure.

The durability properties of the 8FA, 8FASS and 8FAK geopolymer materials were very different. The difference in performance must be linked to different pore structure of these materials. Table 4 presents results of BET nitrogen adsorption analysis, which indicated that the materials had significantly different total porosity, average pore diameters and BET surface areas [15]. The 8FA specimens had a porosity of 17.5%, while 8FASS and 8FAK had 0.36% and 1.98%, respectively. The average pore diameter was found to be ~ 45, ~ 63 and 116 Å in 8FA, 8FASS and 8FAK specimens, respectively. The BET surface area was measured ~ 43 $m^2/g$ in 8FA and only ~ 14 $m^2/g$ in 8FASS and 8FAK specimens. These results correlate well with the performance of the materials in sulfuric acid solution, where 8FA specimen having the smallest pore diameter had better resistance than the 8FASS and 8FAK materials despite its high porosity. The 8FAK samples with the largest average pore diameter had a poor durability in sulfuric acid solution, but were rather durable in the acetic acid solution. This discrepancy is possibly connected to different products of reaction with the acid solutions. In case of sulfuric acid, Na–P1 zeolite (gismondine) formed, while in a solution of acetic acid, amorphous products were produced. Possibly, increased formation of Na–P1 zeolite caused a loss of strength in 8FAK specimens in sulfuric acid solution. Previously, Brough et al.[16] reported a loss of strength in alkali-activated blends with high content of FA, which was attributed to phase transformations in zeolites. Performance of 8FAK and 8FASS geopolymer specimens was significantly better in acetic acid than in sulfuric acid solution possibly due to higher strength of the sulfuric acid solution of pH 0.8 compared to the acetic acid solution of pH 2.4.

OPC specimens did not perform well in both sulfuric and acetic acid solutions. The severe deterioration of OPC samples in acidic environment is connected to the chemical composition with high calcium content (Table 1) and relatively large pore size in the OPC paste at w/c = 0.4 (Table 4). OPC, OPC + FA and 8FA specimens had very similar porosity measured by BET, but their performance in durability tests was very different: The geopolymer specimens 8FA were the most durable, while OPC specimens were the least durable in the acidic environment. The specimens had significantly different median pore sizes: ~ 45, ~ 82 and ~ 100 Å, respectively, in 8FA, OPC + FA and OPC specimens. Thus, the median pore size was of more importance for the durability in acidic solutions than the total porosity. The chemistry of the material was undoubtedly very important for its durability. Geopolymer specimens with very low Ca content performed significantly better than OPC specimens. Among geopolymer and OPC materials, the 8FA material performed significantly better than others, although 8FA specimens had the highest porosity among the geopolymer materials. The good performance of the 8FA material was possibly due to a stable cross-linked aluminosilicate structure and the small, nanometer-sized pores contained in this material.

Table 4
Results of BET nitrogen adsorption analysis

| Specimen | BET surface area ($m^2$/g) | Average pore diameter (4V/A by BET) (Å) | Total porosity (%) |
|---|---|---|---|
| 8FA | 42.9 | 45.2 | 17.5 |
| 8FAK | 14.2 | 116 | 3.13 |
| 8FASS | 13.8 | 62.8 | 1.67 |
| Portland cement paste, w/b = 0.4 | 41.6 | 100.1 | 16.6 |
| Portland cement + FA paste, w/b = 0.4 | 44 | 82.5 | 18 |

The peculiarities of the aluminosilicate structure of the geopolymers are possibly responsible for their different performance in the tests. The active centres on the surface of the alumina silicate gel influence its reactions with the aggressive media. Evidently, the introduction of potassium ions created active sites in 8FAK material that caused its susceptibility to reaction with the sulfuric acid solution and rapid deterioration in this medium. The difference in the effects of the two acid solutions on 8FAK material may also be due to the difference in the anions of acids used in the test. In the acetic acid, the reactions in 8FAK samples produced amorphous polymers that ensured good durability, while in the sulfuric acid, precipitation of Na–P1 zeolite occurred, which was associated with the loss of strength. However, chemistry is not the only factor that affects properties. Morphology is also important for the durability performance of the materials. XRD results suggested different degrees of intrinsic ordering in the 8FA, 8FASS and 8FAK geopolymer samples. The presence of traces of poorly crystalline zeolites in 8FA showed that there were regions of the ordered structures in this material. High durability of the 8FA samples in sulfuric acid solution was attributed to the presence of cross-linked polymer structures that successfully resisted the attack. In the 8FASS sample, only amorphous phases were present. In solutions of both acids, the 8FASS samples initially rapidly lost strength; in the case of acetic acid, the strength loss was stabilised; and in sulfuric acid, the loss of strength was continuous. Chemical stability of the polymers is improved when intrinsic order is present in one or all phases. This observation appeared to be correct for a wide range of polymeric materials, including organic and inorganic polymers and minerals.

Fluctuations of strength in the 8FASS and 8FA specimens in acetic acid solution may be linked to migration of alkalis from geopolymers into solutions. Very significant fluctuations of strength, which were observed in geopolymer specimens immersed in sulfate solutions, were linked to migration of alkalis from geopolymers into solution [17]. Instability of strength is a serious issue for geopolymer materials used in structural applications and additional research is needed to investigate this problem.

SEM observations show that geopolymer materials may have different mode of deterioration. Deterioration may occur through formation of fissures in the amorphous polymer matrix or through crystallisation of zeolites in the amorphous matrix. In this study, the first type of deterioration was characteristic of high-performance materials, and the second type was characteristic of low-performance materials. It is likely that the fissures formed as a result of disintegration of the aluminosilicate gel in the aggressive media, due to breaking of Si–O–Si and Si–O–Al bonds in the polymer. No indication of expansive reaction was observed. The geopolymer materials, which did not perform well in the aggressive environment formed zeolites and grains that caused significant loss of strength due to low intercrystalline bond strength.

## 5. Conclusions

The deterioration of geopolymer materials in acidic media is connected to depolymerisation of aluminosilicate polymers and liberation of silicic acid, replacement of Na and K cations by hydrogen or hydronium ion and dealumination of the geopolymer structure. It is also connected to condensation of siliceous polymers and zeolites, which in some cases lead to a significant loss of strength.

In acidic environment, high-performance geopolymer materials deteriorate with the formation of fissures in amorphous polymer matrix, while low-performance geopolymers deteriorate through crystallisation of zeolites and formation of fragile grainy structures.

The materials tested had a significant difference in the degrees of intrinsic ordering within the polymer gel. The 8FA sample had more ordered structure and the smallest average pore diameter than 8FASS and 8FAK samples. The 8FA specimens had the best resistance in sulfuric acid solution. Introduction of potassium hydroxide in 8FAK samples caused an increase of the average pore diameter and reduced its durability in sulfuric acid solution.

Stability of geopolymer materials in aggressive environments depends on the intrinsic ordering present within aluminosilicate gel. More crystalline geopolymer material prepared with sodium hydroxide was more stable in the aggressive environment of sulfuric and acetic acid solutions than amorphous geopolymers prepared with the sodium silicate activator. The chemical instability would also depend on the presence of the active sites on the aluminosilicate gel surface, which appeared to increase in presence of K ions.

Instability of strength in some geopolymers is of concern in their use as a construction material, and careful consideration should be given to this aspect.

## Acknowledgements

The author is grateful to the Australian Research Council for financial support under Grant DP0209501 and to Civil Engineering Department and School of Physics and Materials Engineering, Monash University, for providing access to equipment used in this investigation.

## References

[1] W.H. Harrison, Durability of concrete in acidic soils and waters, Concrete 1 (2) (1987) 18–24.
[2] T. Bakharev, J.G. Sanjayan, Y.-B. Chen, Resistance of alkali-activated slag concrete to acid attack, Cem. Concr. Res. 33 (2003) 1607–1611.
[3] J. Davidovits, Properties of geopolymer cements, Proceedings of the First International Conference on Alkaline Cements and Concretes, vol. 1, SRIBM, Kiev, Ukraine, 1994, pp. 131–149.
[4] J. Davidovits, Mineral polymers and methods of making them, US Patent 4349386, 1982.
[5] J. Davidovits, Synthetic mineral polymer compound of the silicoaluminates family and preparation process, US Patent 4472199, 1984.
[6] T. Bakharev, Geopolymer materials prepared using class F fly ash and elevated temperature curing, Cem. Concr. Res. (2004) (in press).
[7] A. Palomo, M.W. Grutzeck, M.T. Blanco, Alkali-activated fly ashes a cement for the future, Cem. Concr. Res. 29 (1999) 1323–1329.
[8] J.C. Swanepoel, C.A. Strydom, Utilisation of fly ash in a geopolymeric material, Appl. Geochem. 17 (2002) 1143–1148.
[9] J.G.S. van Jaarsveld, J.S.J. van Deventer, The effect of metal contaminants on the formation and properties of waste-based geopolymers, Cem. Concr. Res. 29 (1999) 1189–1200.
[10] D.W. Breck, Zeolite Molecular Sieves: Structure, Chemistry and Use, Wiley-Interscience, New York, 1974, pp. 415–418.
[11] V.I. Babushkin, G.M. Matveyev, O.P. Mchedlov-Petrossyan, Thermodynamics of Silicates, Springer-Verlag, Berlin, 1985, pp. 276–281.
[12] H. Xu, J.S.J. Van Deventer, The geopolymerisation of alumino-silicate minerals, Int. J. Miner. Process. 59 (2000) 247–266.
[13] W.M. Hendricks, A.T. Bell, C.J. Radke, Effect of organic and alkali metal cations on the distribution of silicate anions in aqueous solutions, J. Phys. Chem. 95 (1991) 9513–9518.
[14] R.K. Iller, The Colloid Chemistry of Silica and Silicates, Cornell Univ. Press, Ithaca, NY, 1955, pp. 27–37.
[15] T. Bakharev, Effect of curing regime and type of activator on properties of alkali-activated fly ash, 1st International Symposium on Nanotechnology in Construction, Paisley, Scotland, June, 2004 (in press).
[16] A.R. Brough, A. Katz, T. Bakharev, G.-K. Sun, R.J. Kirkpatrick, L.J. Struble, J.F. Young, Microstructural aspects of zeolite formation in alkali activated cements containing high levels of fly ash, in: S. Diamond, et al. (Ed.), Microstructure of Cement Based Systems/Bonding and Interfaces in Cementitious Materials, Mater. Res. Soc. Proc., vol. 370, 1996, pp. 199–208.
[17] T. Bakharev, Durability of geopolymer materials in sodium and magnesium sulfate solutions, Cem. Cancr. Res. (in press).